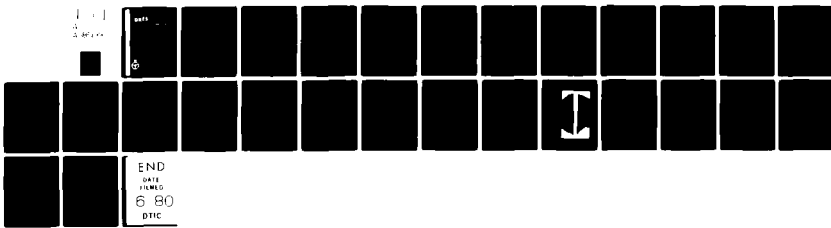
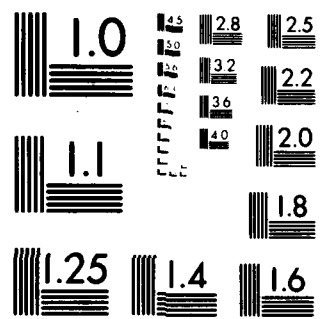


AD-A085 199 DEFENCE RESEARCH ESTABLISHMENT SUFFIELD RALSTON (ALBERTA) F/6 20/8
DIE SWELL FOR NEWTONIAN FLUIDS. (U)
MAY 80 C L CHENIER, G A HILL

UNCLASSIFIED DRES-TN-477

NL





MICROCOPY RESOLUTION TEST CHART
NATIONAL BUREAU OF STANDARDS 1963 A

LEVEL

3

UNCLASSIFIED

UNLIMITED
DISTRIBUTION

DRES

SUFFIELD TECHNICAL NOTE

NO. 477

ADA 085199

DIE SWELL FOR NEWTONIAN FLUIDS (U)

by

C.L. Chenier and G.A. Hill

PCN 13E01

May 1980



UNCLASSIFIED

**UNLIMITED
DISTRIBUTION**

DEFENCE RESEARCH ESTABLISHMENT SUFFIELD
RALSTON ALBERTA

SUFFIELD TECHNICAL NOTE NO. 477

DIE SWELL FOR NEWTONIAN FLUIDS (U)

by

C.L. Chenier and G.A. Hill

PCN 13E01

WARNING

The use of this information is permitted subject to recognition
of proprietary and patent rights.

UNCLASSIFIED

UNCLASSIFIED

DEFENCE RESEARCH ESTABLISHMENT SUFFIELD
RALSTON ALBERTA

SUFFIELD TECHNICAL NOTE NO. 477

DIE SWELL FOR NEWTONIAN FLUIDS (U)

by

C.L. Chenier and G.A. Hill

Accession No.	NP15-00000
DDC Ref.	
Uncontrolled	
Justification	
By	
Classification	
Approved by	
Date	
<i>A</i>	

ABSTRACT

→ The swelling and shrinking of Newtonian jets issuing from circular orifices or slits has been examined. Equations predicting die swell ratio and downstream flow characteristics are developed. The scatter of experimental data has been studied and the factors contributing to this phenomenon are presented. The die swell ratios and jet shapes versus Reynolds numbers for Newtonian liquids are empirically shown.

(U)

UNCLASSIFIED

UNCLASSIFIED

DEFENCE RESEARCH ESTABLISHMENT SUFFIELD
RALSTON ALBERTA

SUFFIELD TECHNICAL NOTE NO. 477

DIE SWELL FOR NEWTONIAN FLUIDS (U)

by

C.L. Chenier and G.A. Hill

INTRODUCTION

The physical characteristics of liquids can greatly affect the performance of mechanical devices used to transport, store or disseminate them. For example, many liquids when thickened by polymers undergo not only viscosity changes which greatly affect their flow properties but also become viscoelastic in nature which can have considerable effect on their transient flow properties.

One method which has considerable use in the measurement of 'elasticity' involves simply pushing the liquid in question out of the end of a small diameter tube. For some non-Newtonian liquids it was observed a long time ago (1) that this could result in jets with diameters considerably larger than the original diameter of the tube or slit. Although this phenomenon has been given several names, the term most commonly used is "die swell". Die swell was considered for over half a

UNCLASSIFIED

century to be due solely to the elastic properties of non-Newtonian liquids. However, in 1961, Middleman and Gavis (2) observed the same phenomenon for Newtonian liquids. They found that for flows below Reynolds number 16 the jets expanded in diameter, whereas at higher Reynolds numbers they contracted. This expansion and contraction was somewhat less than that observed for most viscoelastic liquids but was still significant and was unaccounted for in any theory at that time. In the same report, they attempted to account for this phenomenon by an overall mass and momentum balance between the tube exit and an arbitrary distance downstream where it was assumed the velocity profile was flat and the pressure was atmospheric. Their analysis showed that the swelling effect was due to the relaxing axial velocity profile at the tube exit and to surface tension, although Gavis (3) later pointed out an error in this analysis which showed surface tension did not contribute to the swelling phenomenon.

THEORY

Since the initial discovery of die swell for Newtonian liquids there have been several more theoretical interpretations of this phenomenon. Richardson (4) performed an overall momentum balance but failed to include any terms other than the velocity integrals in his expression for the die swell ratio. Only recently has the die swell phenomenon been accurately predicted using numerical techniques (5,6). In these analyses, the inclusion of the singularity boundary condition at the die exit seems to preclude any hope of a successful analytical solution.

The overall mass and momentum balance on a jet issuing from a slit or tube provides much useful information on the die swell phenomenon. Consider the jet depicted in Figure 1. If we assume a flat velocity profile downstream and atmospheric pressure across the jet, the mass balance between position 0 and position 1 gives (Cartesian coordinates):

$$2\rho \int_0^{Y_0} u dy = 2\rho U_\infty Y_\infty \dots \dots \dots \dots \dots \dots \quad (1)$$

... and the momentum balance gives:

... where it has been assumed that gravitational and surface tension forces are negligible. Some algebraic manipulation of these two complete equations gives a more complete equation for the die swell ratio than given by Richardson (4):

$$\chi = Y_\infty / Y_0 = \frac{\rho \left\{ \int_0^1 u dy \right\}^2}{\rho \int_0^1 u^2 dy + \int_0^1 pdy + \int_0^1 \tau_{xx} dy} \quad \dots \dots \quad (3)$$

... where the integrals have all been normalized by Y_0 . The above equation implies that the final die swell ratio is determined completely by the conditions at the end of the slit provided the assumptions of negligible gravity and surface tension effects are correct. If the last two terms of the denominator of Equation 3 are negligible, then clearly the largest value that the die swell ratio could have would be 1.0. Thus, unless these terms provide a net negative value to the denominator there can be no swelling. With all the above assumptions and further assuming that the velocity profile remains parabolic right up to the slit exit, the velocity integrals in Equation 3 yield a value of 0.833 for the die swell ratio from a slit. Similarly, the die swell ratio for flow from a tube can be calculated as 0.866. These limiting conditions are approached at high Reynolds number flows (2) where numerical simulations have predicted the velocity profiles at the slit exit remain very nearly parabolic (6).

The fact that the velocity profile is affected by the Reynolds number has been demonstrated experimentally. Goulden and MacSporran (7) used a laser anemometer to measure velocity profiles in viscoelastic liquids over a range of Reynolds numbers. At higher Reynolds numbers, their plots demonstrated that longer distances downstream are required before the axial velocity profiles become flat. The reason for this phenomenon

can be understood from an analysis of the axial momentum equation (x-direction) at steady state:

$$u \frac{\partial u}{\partial x} + v \frac{\partial u}{\partial y} = - \frac{\partial \phi}{\partial x} + v \left(\frac{\partial^2 u}{\partial y^2} + \frac{\partial^2 u}{\partial x^2} \right) \dots \dots \dots \quad (4)$$

This equation is non-dimensionalized using the technique of Bird et al. (8) which requires multiplication by a distance term and division by a velocity term. This combination is arbitrarily chosen to be $2Y_0/U_0^2$ and the dimensionless parameters are:

$$\begin{aligned} x' &= x/2Y_0, \quad y' = y/2Y_0, \quad u' = u/U_0 \\ v' &= v/U_0, \quad \phi' = \phi/U_0^2, \quad Re = 2Y_0 U_0 / v \end{aligned} \dots \dots \dots \quad (5)$$

Substituting 5 into 4 gives:

$$u' \frac{\partial u'}{\partial x'} + v' \frac{\partial u'}{\partial y'} = - \frac{\partial \phi'}{\partial x'} + \frac{1}{Re} \left(\frac{\partial^2 u'}{\partial x'^2} + \frac{\partial^2 u'}{\partial y'^2} \right) \dots \dots \dots \quad (6)$$

The individual terms in Equation 6 are now analyzed for the die swell problem making appropriate assumptions. For die swell, the flow remains almost parabolic right up to the tube exit for Reynolds numbers greater than about 10, as has been shown by numerous experimental and theoretical evaluations (4,5,6,7). At the slit exit, although the velocity does begin to relax, it is highly probable that the transverse velocity differentials are much greater than the axial ones, so that:

$$\frac{\partial^2 u'}{\partial y'^2} = -0.75 \gg \frac{\partial^2 u'}{\partial x'^2} \dots \dots \dots \dots \dots \quad (7)$$

... for a parabolic velocity profile at the exit. The pressure gradient for laminar flow in a slit is:

$$\frac{\partial \phi}{\partial x} = - \frac{3vU_0}{Y_0^2} \dots \dots \dots \dots \dots \quad (8)$$

... or in dimensionless form:

It is not obvious that the pressure gradient at the die swell exit is the same as it is upstream; however, it is intuitively obvious that it will be much less at the exit and probably is some small fraction, f , of what it is upstream:

With these assumptions, the terms on the right hand side of Equation 4 are inversely proportional to the Reynolds number:

Thus the terms on the left hand side of Equation 4 must also be inversely proportional to the Reynolds number. If the profile remains parabolic, then only the partial derivative $\partial u' / \partial x'$ can vary. Thus $\partial u' / \partial x'$ must be inversely proportional to the Reynolds number, and for high Reynolds number flows $\partial u' / \partial x'$ will be small and high values of x' (long distances downstream) will be required to achieve a flat profile. Similarly, at low Reynolds numbers $\partial u' / \partial x'$ will be high and smaller distances downstream will be required to achieve a flat profile.

It must be pointed out that this analysis used assumptions which appear to be upheld by experimental and theoretical evidence. At very low Reynolds numbers, however, the velocity profile may vary significantly from parabolic and this analysis should not be expected to hold.

EXPERIMENTAL.

Die swell experiments were conducted to complement and extend the available published data. The experiments were conducted at room temperature with the apparatus depicted in Figure 2. A large tank was pressurized sufficiently to force the liquid through the tube at the

desired flow rate (calculated by the Hagen-Poiseuille equation). This tank was then disconnected from the pressure source to eliminate spurious pressure fluctuations. The liquid to be pumped was maintained in a 0.15 litre or 4.5 litre stainless steel reservoir depending on the volume of liquid required. The flow rate was regulated with a micrometer needle valve and monitored with a rotameter. The rotameter served only to ensure that a constant flow rate was being maintained. The actual flow rate was determined for each experiment by collecting an arbitrary mass of liquid over a measured time interval. This was the simplest procedure due to the impracticality of calibrating every rotameter for every liquid. The liquid jets issuing from the tubes were photographed with a 35 mm camera using either a microscope for very small jets or a camera bellows for larger jets. The light source was located behind the jet, resulting in photographs similar to that shown in Figure 3. Glass rods of known diameter were also photographed in this manner to ensure that no errors in diameter measurements were resulting from unknown optical effects. The diameters of the jets and glass rods were calculated with reference to the known outside diameters of the hypodermic tubes. The glass rod experiments demonstrated that the technique was accurate to within 0.5% of the true diameter. The diameter measurements were made from enlarged glossy prints using a calibrated magnifier lens.

The Newtonian liquids used in these experiments consisted of mixtures of glycerol and water. The concentrations, densities (measured with pycnometers), and viscosities (Canon-Fenske) are listed in Table 1. The room temperatures at which the die swell experiments and physical measurements were made are also listed in Table 1.

The tubes used in these experiments were stainless steel hypodermic needles. Their ends were carefully ground using a carborundum stone and fine grade crocus cloth. The inside edges of the orifices were smoothed and deburred with stilettos. Ten different tubes were used in these experiments and their characteristics are listed in Table 2. Diameters were measured under a microscope in three different cross-sections to ensure circularity as listed in Table 2. The ends of the

tubes were tapered from their outside diameters to their inside diameters (as shown in Figs. 2 and 3) in order to reduce the tendency of the liquid to spread along the orifice edge. The lengths of the tubes were several factors larger than their diameters as listed in Table 2. This reduced the effect of entrance phenomena on the die swell measurements (9).

RESULTS AND DISCUSSION

The experimental data for the die swell ratio are listed in Table 3 as a function of Reynolds number and plotted in Figure 4 (triangles). The solid lines on this graph represent an envelope of the original data gathered by Middleman and Gavis (2). The circles indicate the data of Goren and Wronski (10) and the crosses indicate the extremes of the data gathered by Gavis and Modan (9). The data gathered by all investigators show considerable amounts of scatter.

The causes for this experimental scatter are a combination of many factors some of which are listed below.

(i) The actual measurement process off the photographs can yield results which vary from investigator to investigator. In one study here, it was found that two separate investigators using two different measuring devices (a graduated magnifier and a steel machinist's scale) produced data that was generally within a range of $\pm 1.0\%$ of the actual percentage die swell, but differences as high as $\pm 3.0\%$ were observed. This could account for much of the scatter of our own data and probably contributes to the scatter of others.

(ii) Gavis and Modan (9) found that the length to diameter ratio of the tube affected the jet shrinkage at Reynolds numbers greater than 16 but they could not find any correlation at lower Reynolds numbers. We avoided this phenomenon to a large extent by employing tubes with length to diameter ratios 9 or greater.

(iii) Although the original investigators (2) indicated that surface tension contributed to die swell, Gavis (3) showed theoretically that this was incorrect and Goren and Wronski (10) could not find any experimental proof of this phenomenon. Reddy and Tanner's numerical prediction (5) also indicated that surface tension had little effect at the Reynolds numbers studied here.

(iv) Goren and Wronski (10) speculated that viscous heating in the capillary could result in distorted velocity profiles and incorrect die swell ratios. This effect would also tend to decrease the liquid viscosity and increase the Reynolds number.

(v) Goren and Wronski (10) also speculated that air friction on the jet could be considerable at higher Reynolds numbers and this could increase the die swell ratios considerably.

(vi) Most investigators have tried to avoid the effects of gravity on their experiments by either shooting their jets horizontally and considering only the shapes before the jets began to curve downwards or by shooting their jets into a non-soluble liquid of similar density. However, Hill (6) has numerically predicted that for small diameter tubes, as used in most experimental work, gravity has negligible effect in the axial direction.

To test the effect of tube diameter on the die swell ratio a series of experiments were conducted using tubes of various diameters and liquids of various viscosities. All runs were made at Reynolds number 7.0 and the data are listed at the top of Table 3. The results of these tests are plotted in Figure 5. This graph demonstrates that there is no consistent effect of tube diameter on the die swell ratio. Also, because of the random location of the various viscosity liquids for each tube, it was concluded that viscous heating was not a factor contributing to scatter at this flow rate. Rather, the measured die swell ratios appear to be affected by some individual characteristics of each tube. This is noticeable by the fact that some tubes yielded consistently higher ratios than other tubes. One tube resulted in swelling of 12% to 19% whereas most of the data varied from 7% to 10%. Upon close microscopic

examination of this tube, it was discovered that a slight taper existed around the inside circumference. This resulted in an expansion affect on the liquid before it even reached the end of the tube. Calculations showed this taper resulted in an exit diameter 9% greater than the tube diameter and this accounts for the unusually large die swell ratios measured from this tube. None of the data gathered from this tube was used in Figure 4. Allan (11) has numerically predicted the effects of tapers on the die swell ratio for creeping flow and our experimental results would seem to confirm his prediction. The shape of the orifice is therefore very critical to experimental measurements of die swell and undoubtedly plays a big role in the scatter of experimental data. Six various possible configurations of the orifice shape are shown schematically in Figure 6. As most experimental measurements of die swell are performed on small diameter tubes, the difficulty of achieving the perfect orifice is significant.

Several photographs were examined for jet shapes; the data are listed in Table 4 and depicted in Figure 7. Here again, the large error due to the above mentioned experimental difficulties must be kept in mind. The fact that the low Reynolds number jet shapes do not leave from the tube corner could be due either to slightly tapered orifices or to spreading of the liquid along the orifice edge. In either case, the experimental data still compare favorably to the data of Goren and Wronski (10), who based their calculations on the initial jet diameter and not the tube diameter. The jet shape data also illustrated the fact that high Reynolds numbers required longer downstream distances before flat surface profiles are achieved, as predicted in the theory. At low Reynolds numbers, when $X_0 \approx Y_0$, the jet shape does not keep contracting, however, probably due to the non-parabolic velocity profile at the tube exit.

CONCLUSIONS

The overall mass and momentum balances yield an equation for the die swell ratio which shows that swelling at the tube exit is caused

by a net negative pressure and axial stresses across the tube. The relaxation of axial velocity and surface shape can be shown to be a function of the Reynolds number. At high Reynolds numbers long distances are required downstream before these parameters become completely relaxed.

The experimental measurements of die swell show a large degree of scatter in the data for all investigations. This scatter has been demonstrated to be due primarily to the accuracy of the measurement technique and to the quality of the tube orifices. Due to the importance and ease of this technique for measuring elasticity in non-Newtonian liquids, it would seem profitable to invest time in the design and construction of devices to overcome these present handicaps.

The experimentally measured jet shape data plus the relaxing axial velocity profiles measured by Goulden and MacSporran (7) have demonstrated the correctness of the dimensional analysis which predicts larger downstream distances are required to overcome disturbances at higher Reynolds numbers.

REFERENCES

- (1) Barus, G. Am. J. Sci. 45: 87, 1893.
- (2) Middleman, S. and J. Gavis. Phys. Fluids 4: 355, 1961.
- (3) Gavis, J. Phys. Fluids 7: 1097, 1964.
- (4) Richardson, A. Rheol. Acta 9: 193, 1970.
- (5) Reddy, K.R. and R.I. Tanner. Comput. Fluids 6: 83, 1978.
- (6) Hill, G.A. Numerical Simulation of Free Surface Flows, PhD Dissertation, University of Saskatchewan, 1979.
- (7) Goulden, D.D. and W.C. MacSporan. J. Non-Newtonian Fluid Mech. 1: 183, 1976.
- (8) Bird, R.B., W.E. Stewart and E.N. Lightfoot. Transport Phenomena, John Wiley and Sons Inc., 1960, pp. 107.
- (9) Gavis, S.L. and M. Modan. Phys. Fluids 10: 487, 1967.
- (10) Goren, S.L. and S. Wronski. J. Fluid Mech. 25: 185, 1966.
- (11) Allan, W. Int. J. Num. Methods Eng. II, 1621, 1977.

NOMENCLATURE

p	=	pressure
u	=	axial velocity
U_0	=	average bulk velocity far upstream
U_M	=	maximum axial velocity
U_∞	=	axial velocity far downstream
v	=	transverse velocity
V_M	=	maximum transverse velocity
x	=	axial position
X_0	=	characteristic length downstream
y	=	transverse position
Y_0	=	characteristic length or width across jet
Y_∞	=	jet width far downstream

Greek Symbols

ν	=	kinematic viscosity
ρ	=	density
τ_{xx}	=	axial stress
ϕ	=	pressure variable
x	=	die swell ratio

UNCLASSIFIED

TABLE 1
NEWTONIAN FLUIDS USED

Liquid No.	% Glycerol by Volume	Density (g cm ⁻³)	Viscosity (cm ² s ⁻¹)	Temperature (°C)
1	0	0.997 [†]	0.01	25
2	85.1	1.221	0.79	24
3	87.8	1.231	1.28	25
4	90.5	1.238	1.78	25
5	91.3	1.243	2.39	23
6	91.3	1.242	2.40	23
7	93.8	1.245	2.81	25
8	94.6	1.248	3.84	25

UNCLASSIFIED

[†] CRC Handbook

UNCLASSIFIED

TABLE 2
TUBES USED IN DIE SWELL EXPERIMENTS

Tube No.	Outside Diameter (cm \pm 0.0005)	Inside Diameter (cm \pm 0.0005)	L/D Ratio
1	0.040	0.024	0.023
2	0.072	0.043	0.044
3	0.090	0.058	0.058
4	0.090	0.058	0.058
5	0.089	0.060	0.059
6	0.125	0.085	0.084
7	0.124	0.085	0.084
8	0.165	0.116	0.113
9	0.183	0.132	0.117
10	0.240	0.181	0.176

UNCLASSIFIED

UNCLASSIFIED

TABLE 3
EXPERIMENTAL DIE SWELL DATA

Liquid No.	Tube No.	Reynolds No.	Die Swell x
3	1	7.1	1.07
3,4	2	7.2 - 7.3	1.12 - 1.19
4,7	3	6.9 - 7.4	1.07 - 1.08
4,7	6	6.6 - 7.2	1.09 - 1.11
7,8	8	6.8 - 7.4	1.05 - 1.07
7,8	9	6.7 - 7.2	1.06 - 1.08
8	10	6.3 - 6.9	1.08 - 1.10
5	5	2.27	1.137
5	4	4.00	1.097
5	7	5.26	1.136
5	6	10.65	1.011
2	7	15.4	1.035
2	8	22.1	0.970
2	4	47.0	0.933
3	8	17.9	0.981
3	8	24.0	0.959
3	8	14.8	0.994
3	8	18.1	0.981
2	6	62.5	0.907
2	7	33.8	0.965
2	8	42.6	0.936
2	8	89.9	0.896

UNCLASSIFIED

UNCLASSIFIED

TABLE 4

EXPERIMENTAL JET SHAPE DATA
(DIE SWELL RATIOS)

Distance Downstream x/Y_0	Reynolds Number							
	4.0	7.1	14.8	18.1	24.0	47.0	62.5	89.9
0.00	1.019	1.008	1.016	1.015	1.015	1.011	1.003	0.998
0.40	1.052	1.019	1.000	0.992	0.981	0.978	0.955	0.947
0.80	1.075	1.042	0.994	0.981	0.970	0.956	0.939	0.930
1.20	1.086	1.053	0.994	0.981	0.959	0.944	0.923	0.919
1.60	1.097	1.059	0.994	0.981	0.959	0.939	0.915	0.911
2.00	1.097	1.064			0.959	0.933	0.913	0.908
2.40		1.064				0.933	0.907	0.905
2.80							0.907	0.899
3.00							0.907	0.896

UNCLASSIFIED

UNCLASSIFIED

STN 477

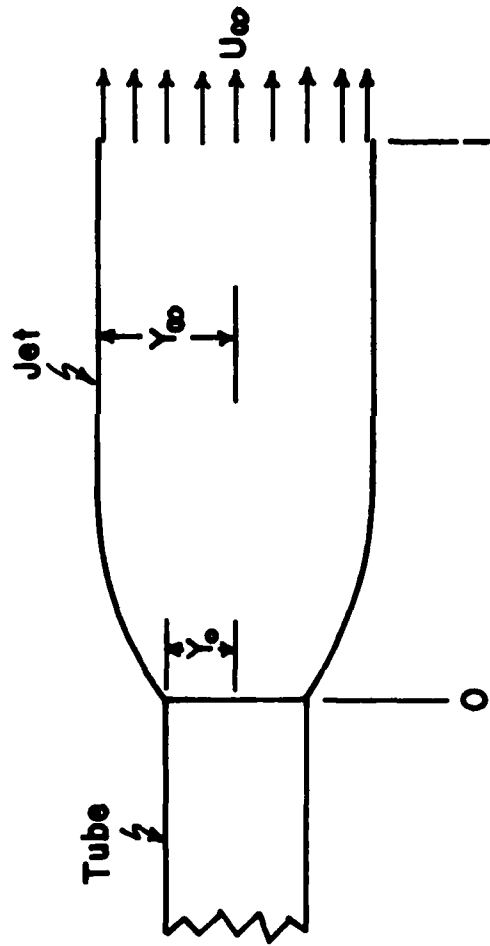


Figure 1. Schematic of a Swelling Jet

UNCLASSIFIED

UNCLASSIFIED

STN 477

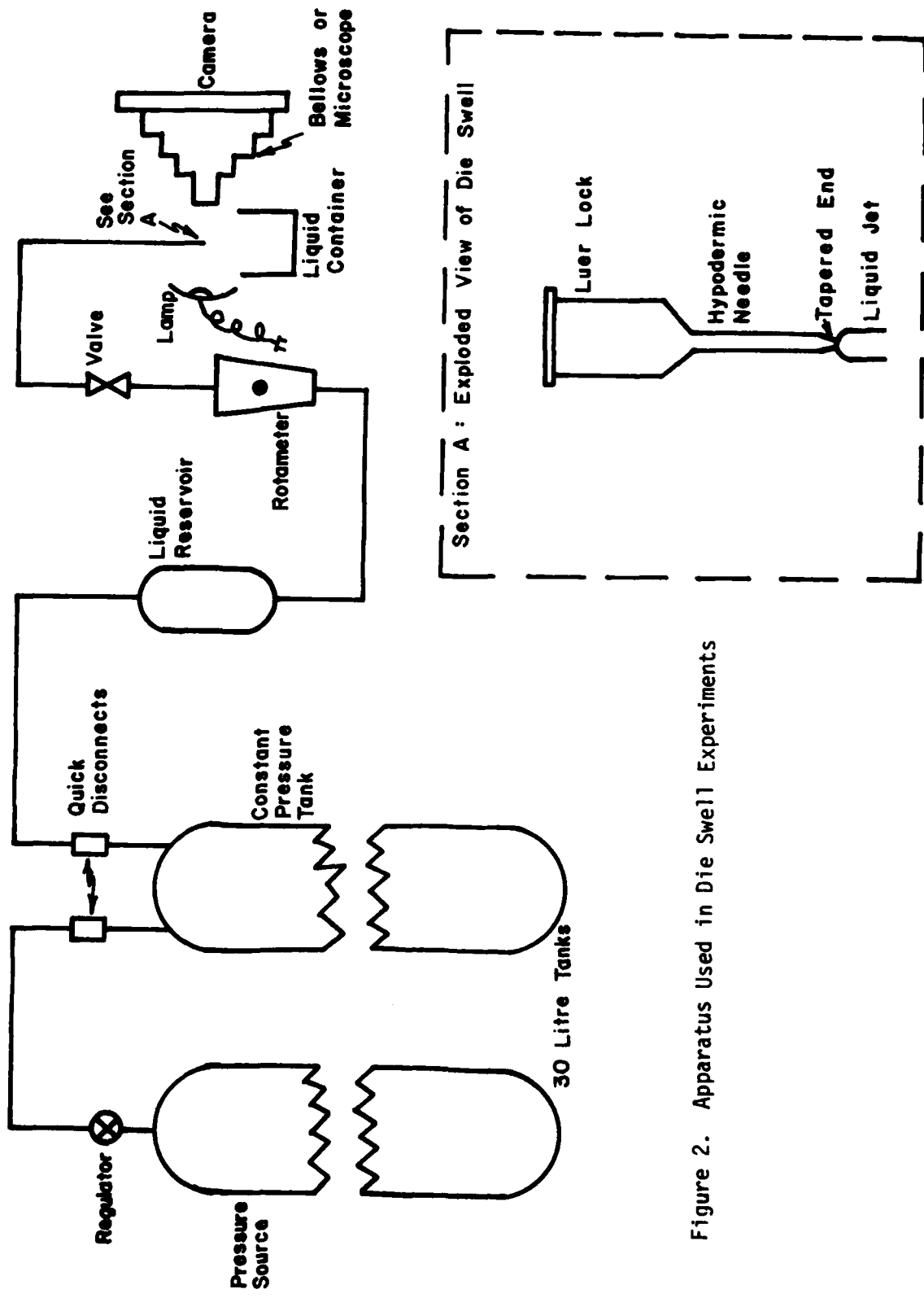


Figure 2. Apparatus Used in Die Swell Experiments

UNCLASSIFIED

UNCLASSIFIED

STN 477

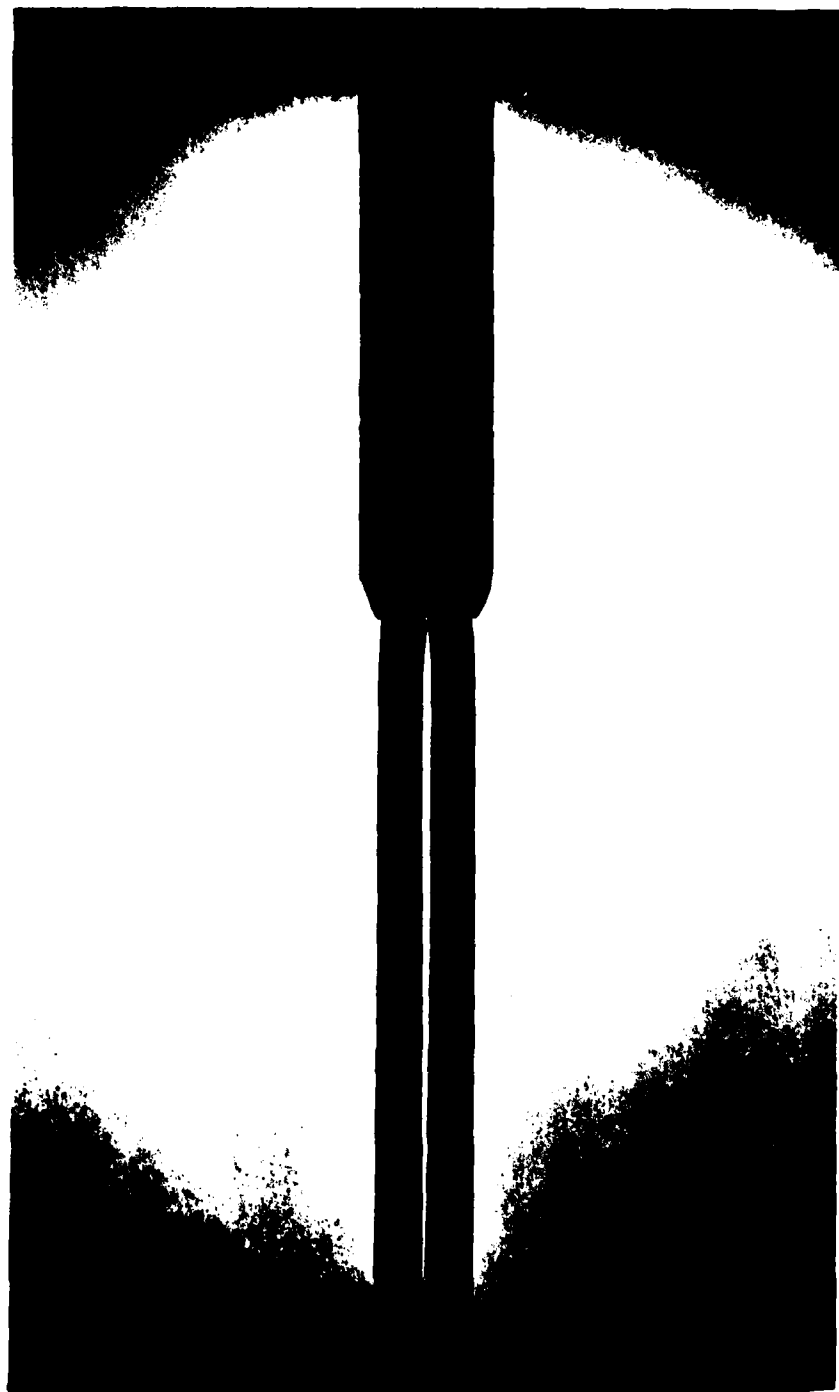


Figure 3. A Typical Die Swell Jet

UNCLASSIFIED

UNCLASSIFIED

STN 477

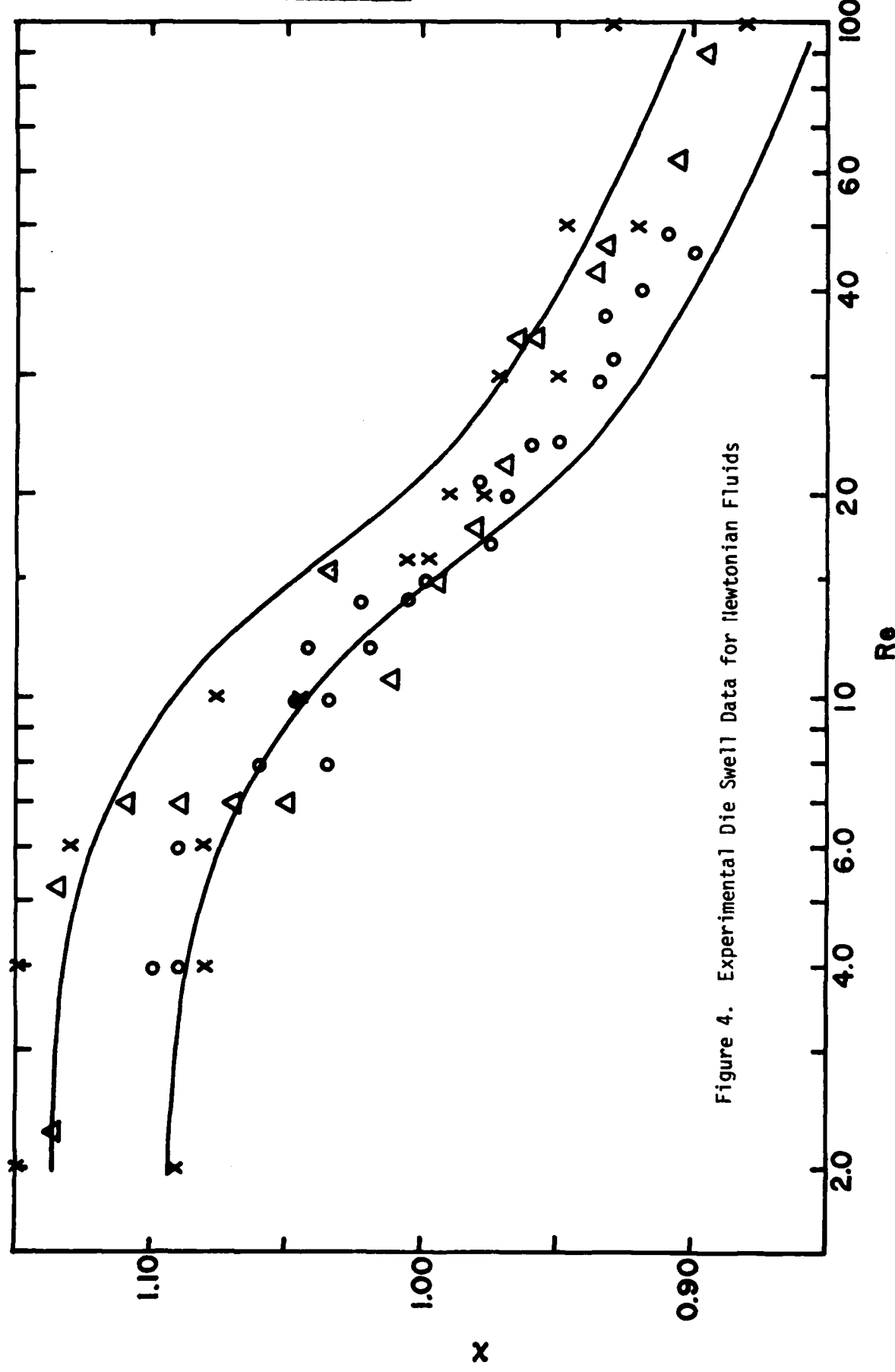
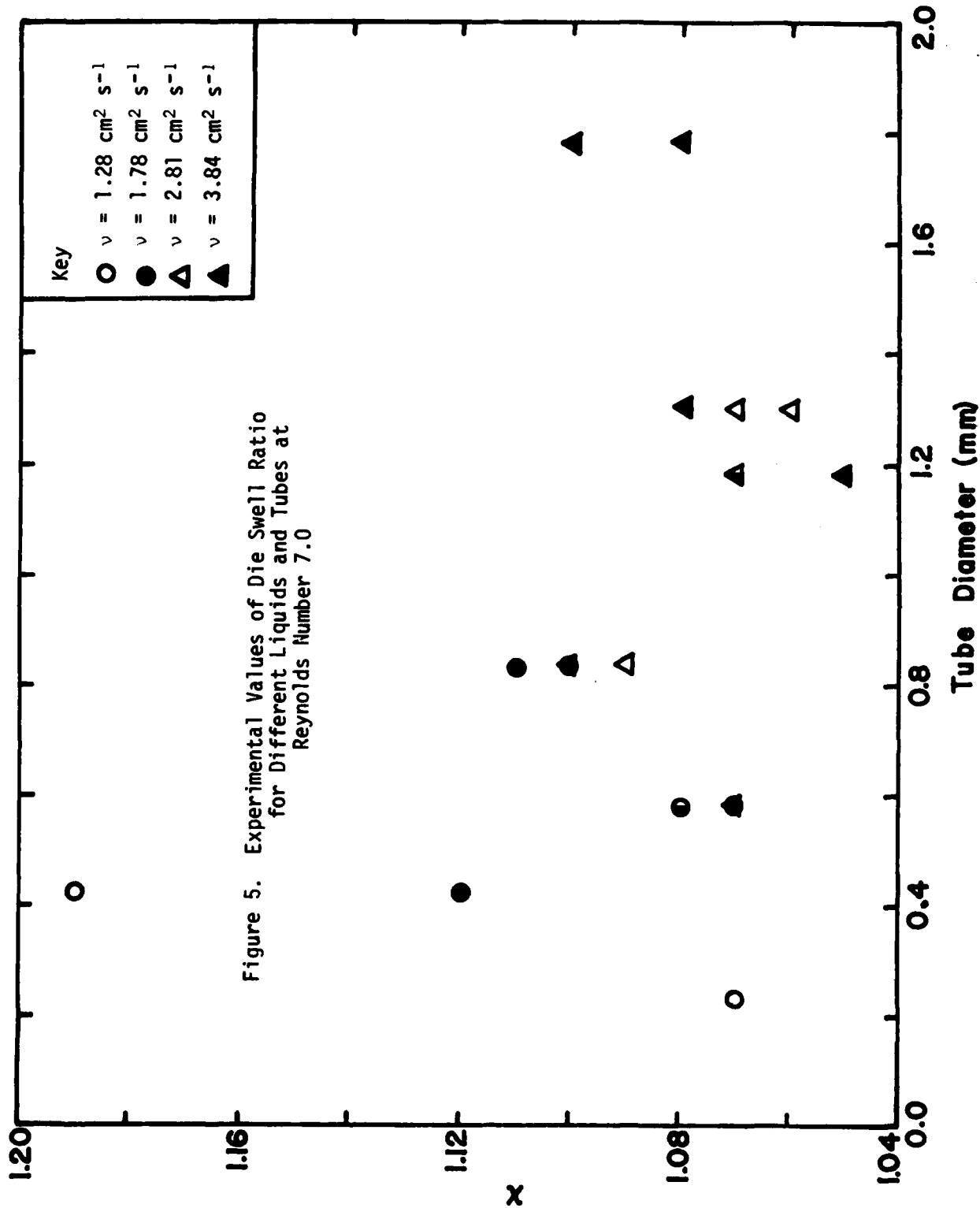


Figure 4. Experimental Die Swell Data for Newtonian Fluids

UNCLASSIFIED

UNCLASSIFIED

STN 477



UNCLASSIFIED

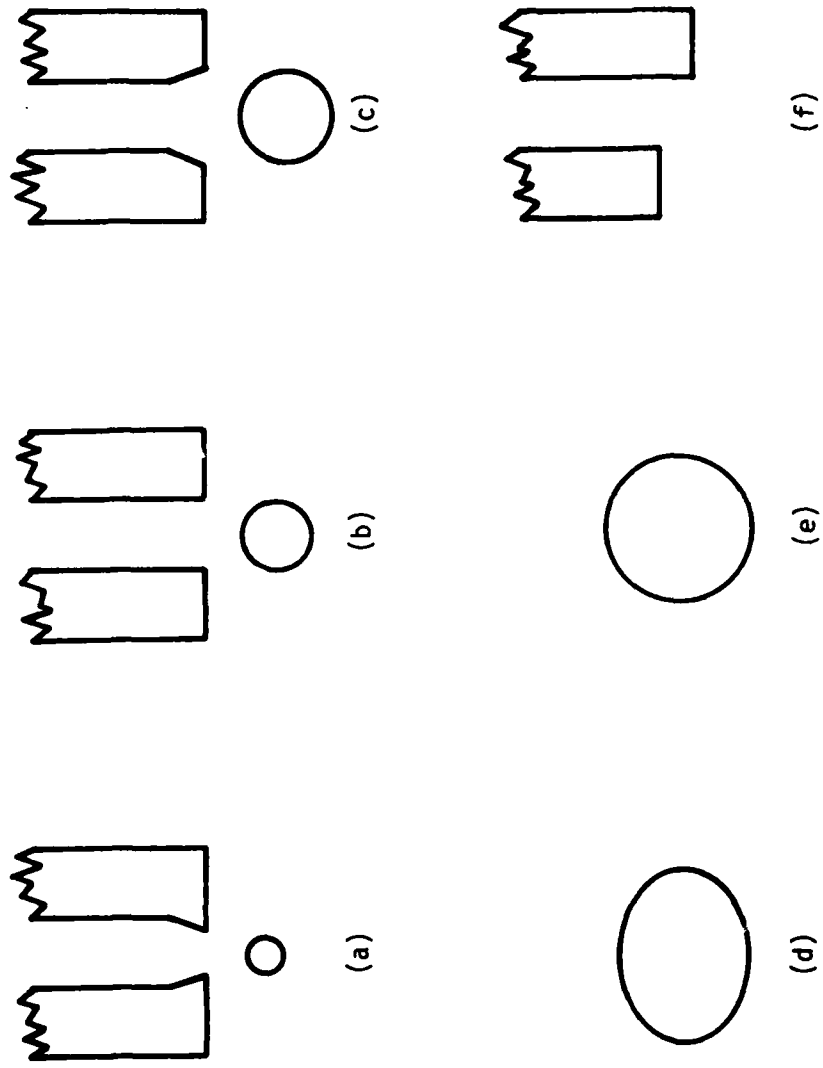


Figure 6. Various Orifice Configurations: (a) tapered in ... die swells too small, (b) straight ... die swells correct, (c) tapered out ... die swells too large, (d) elliptical ... incorrect die swells, (e) circular ... correct die swells, (f) not square ... incorrect die swells

UNCLASSIFIED

STN 477

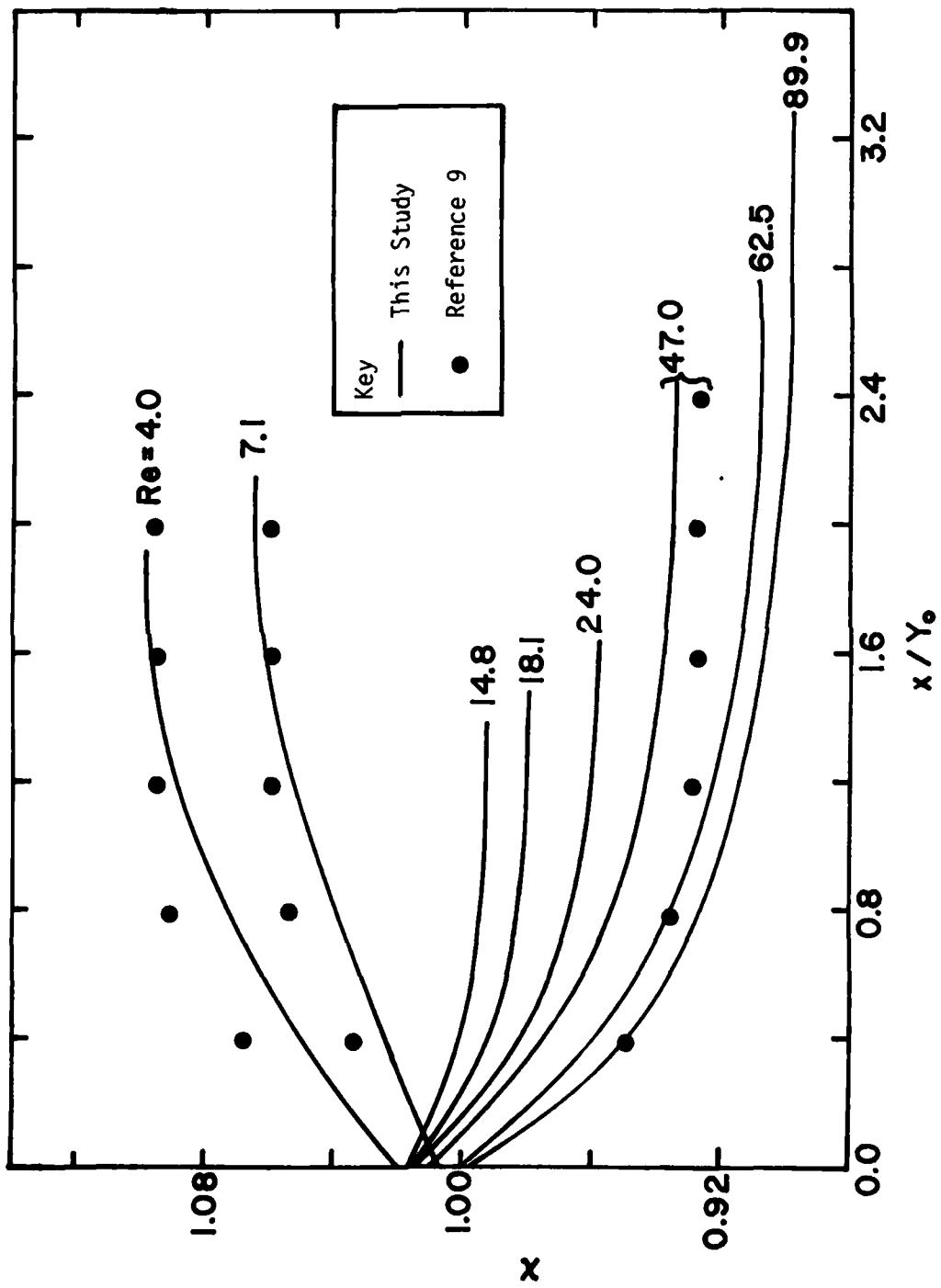


Figure 7. Experimental Jet Shapes

UNCLASSIFIED

UNCLASSIFIED

Security Classification

DOCUMENT CONTROL DATA - R & D

(Security classification of title, body of abstract and indexing annotation must be entered when the overall document is classified)

1. ORIGINATING ACTIVITY DEFENCE RESEARCH ESTABLISHMENT SUFFIELD		2a. DOCUMENT SECURITY CLASSIFICATION UNCLASSIFIED
		2b. GROUP AD-A085199
3. DOCUMENT TITLE b DIE SWELL FOR NEWTONIAN FLUIDS (U)		
4. DESCRIPTIVE NOTES (Type of report and inclusive dates) 7 Technical Note		
5. AUTHOR(S) (Last name, first name, middle initial) Chenier, C.L. and Hill, G.A. 10 C.L. / Chenier G.A. / Hill		
6. DOCUMENT DATE MAY 1980	7a. TOTAL NO. OF PAGES 24	7b. NO. OF KEFS 11
8a. PROJECT OR GRANT NO. PCN 13E01	8b. ORIGINATOR'S DOCUMENT NUMBER(S) SUFFIELD TECHNICAL NOTE NO. 477	
8b. CONTRACT NO.	9b. OTHER DOCUMENT NO.(S) (Any other numbers that may be assigned this document)	
10. DISTRIBUTION STATEMENT UNLIMITED DISTRIBUTION 14 DRES-TN-477		
11. SUPPLEMENTARY NOTES		12. SPONSORING ACTIVITY
13. ABSTRACT The swelling and shrinking of Newtonian jets issuing from circular orifices or slits has been examined. Equations predicting die swell ratio and downstream flow characteristics are developed. The scatter of experimental data has been studied and the factors contributing to this phenomenon are presented. The die swell ratios and jet shapes versus Reynolds numbers for Newtonian liquids are empirically shown. (U)		

DDRS
10-870

403104

J03

KEY WORDS

Liquids

Newtonian

Die Swell

Experimental

Theoretical

INSTRUCTIONS

1. **ORIGINATING ACTIVITY:** Enter the name and address of the organization issuing the document.
2. **DOCUMENT SECURITY CLASSIFICATION:** Enter the overall security classification of the document including special warning terms whenever applicable.
- 2b. **GROUP:** Enter security reclassification group number. The three groups are defined in Appendix 'M' of the DRS Security Regulations.
3. **DOCUMENT TITLE:** Enter the complete document title in all capital letters. Titles in all cases should be unclassified. If a sufficiently descriptive title cannot be selected without classification, show title classification with the usual one-capital-letter abbreviation in parentheses immediately following the title.
4. **DESCRIPTIVE NOTES:** Enter the category of document, e.g. technical report, technical note or technical letter. If appropriate, enter the type of document, e.g. interim, progress, summary, annual or final. Give the inclusive dates when a specific reporting period is covered.
5. **AUTHOR(S):** Enter the name(s) of author(s) as shown on or in the document. Enter last name, first name, middle initial. If military, show rank. The name of the principal author is an absolute minimum requirement.
6. **DOCUMENT DATE:** Enter the date (month, year) of establishment approval for publication of the document.
- 7a. **TOTAL NUMBER OF PAGES:** The total page count should follow normal pagination procedures, i.e., enter the number of pages containing information.
8. **NUMBER OF REFERENCES:** Enter the total number of references cited in the document.
9. **PROJECT OR GRANT NUMBER:** If appropriate, enter the applicable research and development project or grant number under which the document was written.
10. **CONTRACT NUMBER:** If appropriate, enter the applicable number under which the document was written.
11. **ORIGINATOR'S DOCUMENT NUMBER(S):** Enter the official document number by which the document will be identified and controlled by the originating activity. This number must be unique to this document.
- 9b. **OTHER DOCUMENT NUMBER(S):** If the document has been assigned any other document numbers (either by the originator or by the sponsor), also enter this number(s).
10. **DISTRIBUTION STATEMENT:** Enter any limitations on further dissemination of the document, other than those imposed by security classification, using standard statements such as:
 - (1) "Qualified requesters may obtain copies of this document from their defense documentation center."
 - (2) "Announcement and dissemination of this document is not authorized without prior approval from originating activity."
11. **SUPPLEMENTARY NOTES:** Use for additional explanatory notes.
12. **SPONSORING ACTIVITY:** Enter the name of the departmental project office or laboratory sponsor, the research and development. Include address.
13. **ABSTRACT:** Enter an abstract giving a brief and factual summary of the document, even though it may also appear elsewhere in the body of the document itself. It is highly desirable that the abstract of classified documents be unclassified. Each paragraph of the abstract shall end with an indication of the security classification of the information in the paragraph (unless the document itself is unclassified) represented as (TS), (SI), (C), (R), or (U).
The length of the abstract should be limited to 20 single-spaced standard typewritten lines; 7½ inches long.
14. **KEY WORDS:** Key words are technically meaningful terms or short phrases that characterize a document and could be helpful in cataloging the document. Key words should be selected so that no security classification is required. Identifiers, such as equipment model designation, trade name, military project code name, geographic location, may be used as key words but will be followed by an indication of technical context.